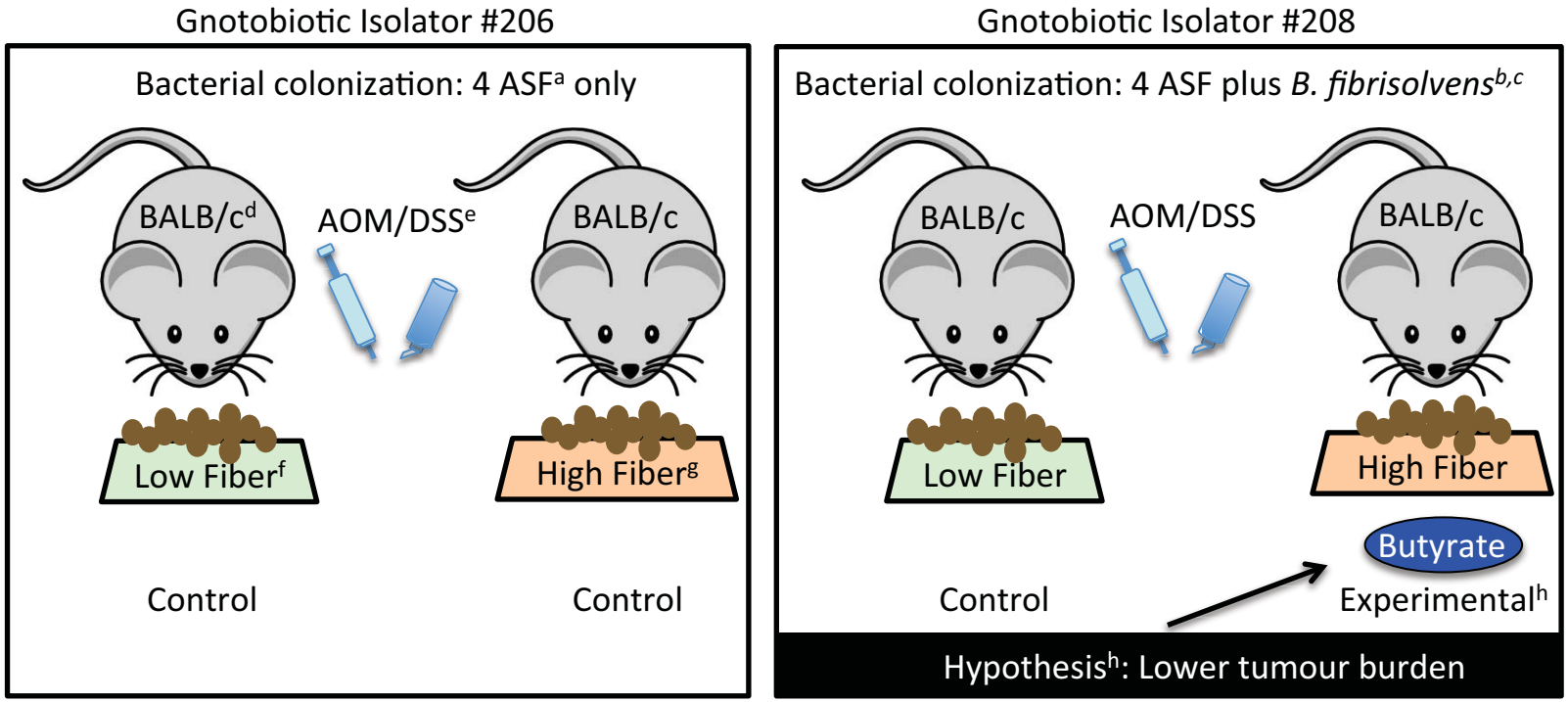

Supplementary Figure 1. Overall experimental design including the rationale behind specific details. **(a)** Mice were colonized with 4 out of the 8 ASF bacterial strains (ASF360, ASF361, ASF457, and ASF519). The other 4 ASF strains (ASF356, ASF492, ASF500, ASF502) were excluded because they are known or suspected (based on their phylogeny[1,2]) butyrate producers that would have prevented the hypothesis from being tested. (**b)** In the first set of experiments, a wild-type (type I) butyrate-producing strain of *B. fibrisolvens* was used (ATCC 19171) as depicted in Gnotobiotic Isolator #208. Subsequently, a mutant (type II) strain (ATCC 51255) that produces 5-10-fold less butyrate was also used. This mutant *B. fibrisolvens* was used in combination with the same 4 ASF strains but in a separate gnotobiotic isolator (not shown). The availability of the mutant strain is what led to the decision to use *B. fibrisolvens* instead of another butyrate producer. In addition, wild-type *B. fibrisolvens* has been associated with decreased aberrant crypt foci in the colon and rectum of mice maintained in conventional (non-gnotobiotic) SPF conditions[7]. **(c)** The decision to polyassociate mice with 4 ASF strains plus *B. fibrisolvens* instead of to monoassociate with *B. fibrisolvens* was based on three considerations. First, the ASF strains were developed at the National Cancer Institute in 1978 to restore normalcy to the GI tract, which is abnormal in germfree and monoassociated mice[4], but in a defined manner as opposed to the undefined microbiota in conventionally-raised mice maintained in a specific pathogen free (SPF) facility. ASF-colonized mice are routinely used in gnotobiotic facilities for this reason. Second, commensal bacteria are required for an inflammatory response following DSS treatment, which is a detergent that breaks down the barrier function of the gut and brings bacteria from the lumen into close physical proximity with inflammatory cells from the lamina propria to induce a colitis-like condition. As a result, DSS often exacerbates tumorigenesis in AOM-treated mice[3,8]. A combination of bacteria is more likely to stimulate significant inflammation. Third, some of the ASF bacteria may crossfeed *B. fibrisolvens* such as by producing acetate to increase butyrate production[5]. **(d)** BALB/c was selected as the mouse strain because it is genetically susceptible to AOM/DSS-induced tumors compared to other inbred strains that have been analyzed[3] (and D.W. Threadgill, unpublished results). (**e)** AOM was administered by i.p. injection, and DSS was administered in the drinking water following standard procedures at the concentrations given in the Methods section. The AOM/DSS model was chosen because it is specifically induces colorectal cancer unlike ApcMin tumors which are almost entirely in the small intestine[3,8]. Moreover, the tumors resemble human CRC tumours with respect to their transcriptome profiles[6] and the mutations that accumulate[3,8]. **(f)** The low-fiber consisted of 2% cellulose to maintain colonic transit. **(g)** The high-fiber diet consisted of 2% cellulose plus 6% FOS/inulin for a total of 8%. FOS/inulin was selected as the fiber source because it is a prebiotic known to be highly fermentable and yield relatively high levels of butyrate (i.e., "butyrogenic"), and this has been implicated in tumor suppression in previous studies of rodent models of CRC maintained in conventional (non-gnotobiotic) SPF facilities[9-12] (although not in other studies[13,14]). **(h)** According to our hypothesis, it is the combination of a high-fiber (prebiotic) diet and *B. fibrisolvens* that will have a protective effect (and is the experimental group) with neither one being chemoprotective on their own (which comprise 2 of 3 control groups).

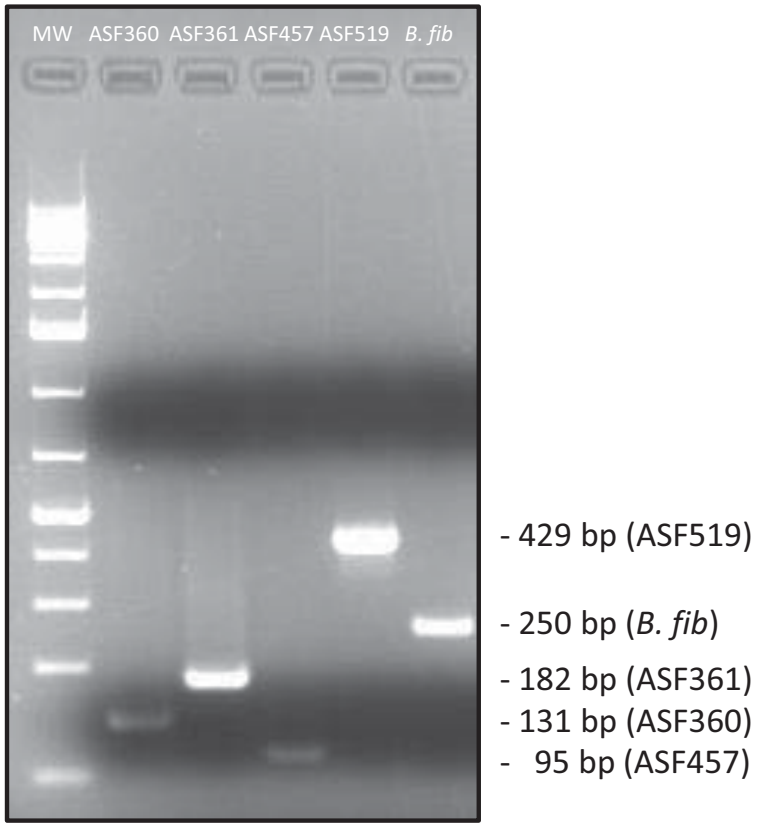

Supplementary Figure 2. Confirmation of the ASF strains and *B. fibrisolvens* by PCR. MW, 1-kb plus molecular weight ladder. PCR product sizes are shown on the right and are compatible with what has been reported previously. The intensity of the PCR products for ASF360 and ASF457 are diminished because of the bromophenol blue dye front.

Low-Fiber Diet (5SRZ)

Mod LabDiet® 5P04 w/Dextrin and Low Fiber — 5SRZ

DESCRIPTION

Modified LabDiet® Laboratory 5P04 (RMH 3500) with dextrin replacing some corn and wheat, and the high fiber ingredients removed.

Storage conditions are particularly critical to TestDiet® products, due to the absence of antioxidants or preservative agents. To provide maximum protection against possible changes during storage, store in a dry, cool location. Storage under refrigeration (2° C) is recommended. Maximum shelf life is six months. (If long term studies are involved, storing the diet at -20° C or colder may prolong shelf life.) Be certain to keep in air tight containers.

*Product Forms Available**	*Catalog #*
1/2" Pellet	1813680

*Other Forms Available On Request

INGREDIENTS

Dehulled Soybean Meal, Wheat, Maltodextrin, Ground Corn, Fish Meal, Soybean Oil, Wheat Middlings, Calcium Carbonate, Brewers Dried Yeast, Dicalcium Phosphate, Salt, Vitamin/Mineral Premix, DL-Methionine, Choline Chloride, L-Lysine, Silicon Dioxide.

NUTRITIONAL PROFILE [1]

Nutrient	Value
Protein, %	***23.1***
Arginine, %	1.47
Histidine, %	0.54
Isoleucine, %	1.15
Leucine, %	1.75
Lysine, %	1.50
Methionine, %	0.69
Cystine, %	0.30
Phenylalanine, %	1.04
Tyrosine, %	0.64
Threonine, %	0.88
Tryptophan, %	0.30
Valine, %	1.18
Alanine, %	1.28
Aspartic Acid, %	2.67
Glutamic Acid, %	4.87
Glycine, %	1.19
Proline, %	1.50
Serine, %	1.24
Taurine, %	0.03
Fat (ether extract), %	***5.7***
Fat (acid hydrolysis), %	***6.4***
Cholesterol, ppm	265
Linoleic Acid, %	2.55
Linolenic Acid, %	0.35
Arachidonic Acid, %	0.01
Omega-3 Fatty Acids, %	0.47
Total Saturated Fatty Acids, %	1.14
Total Monounsaturated Fatty Acids, %	1.20
Polyunsaturated Fatty Acids, %	2.86
Fiber (max), %	***2.1***
Neutral Detergent Fiber[2], %	7.7
Acid Detergent Fiber[3], %	2.8
Nitrogen-Free Extract (by difference), %	***53.2***
Starch, %	41.48
Glucose, %	0.23
Fructose, %	0.07
Sucrose, %	1.03
Lactose, %	0.00
Total Digestible Nutrients, %	**64.4**
Energy (kcal/g) [4]	**3.57**

From:	kcal	%
Protein	0.926	25.9
Fat (ether extract)	0.514	14.4
Carbohydrates	2.129	59.7

Minerals	
Ash, %	**5.8**
Calcium, %	1.17
Phosphorus, %	0.70
Phosphorus (available), %	0.47
Potassium, %	0.80
Magnesium, %	0.18
Sulfur, %	0.27
Sodium, %	0.29
Chloride, %	0.50
Fluorine, ppm	22.1
Iron, ppm	350
Zinc, ppm	110
Manganese, ppm	126
Copper, ppm	14
Cobalt, ppm	0.36
Iodine, ppm	0.99
Chromium, ppm	0.97
Selenium, ppm	0.36

Vitamins	
Carotene, ppm	0.1
Vitamin A, IU/g	30
Vitamin D-3 (added), IU/g	2.2
Vitamin E, IU/kg	74
Vitamin K (as menadione), ppm	1.6
Thiamin Hydrochloride, ppm	90
Riboflavin, ppm	15.0
Niacin, ppm	97
Pantothenic Acid, ppm	30
Folic Acid, ppm	2.8
Pyridoxine, ppm	8.00
Biotin, ppm	0.3
Vitamin B-12, mcg/kg	74
Choline Chloride, ppm	2,000
Ascorbic Acid, ppm	0

1. Based on the latest ingredient analysis information. Since nutrient composition of natural ingredients varies, analysis will differ accordingly. Nutrients expressed as percent of ration on an As-Fed basis except where otherwise indicated. Moisture content is assumed to be 10.0% for the purpose of calculations.
2. NDF = approximately cellulose, hemi-cellulose and lignin.
3. ADF = approximately cellulose and lignin.
4. Energy (kcal/gm) - Sum of decimal fractions of protein, fat and carbohydrate x 4,9,4 kcal/gm respectively.

FEEDING DIRECTIONS

Feed ad libitum. Plenty of fresh, clean water should be available at all times.

CAUTION:
Perishable - store upon receipt.
For laboratory animal use only; not for human consumption.

9/2/2009

ISO 9001:2000 CERTIFIED

TestDiet
www.testdiet.com

High-Fiber Diet (5SVL)

Mod. 5P04 w/ Maltodextrin, Inulin and Fructo-Oligosaccharides — 5SVL

DESCRIPTION

Modified LabDiet® ProLab 3500 (5P04) with Maltodextrin and Inulin/Fructo-Oligosaccharides Mixture.

Storage conditions are particularly critical to TestDiet® products, due to the absence of antioxidants or preservative agents. To provide maximum protection against possible changes during storage, store in a dry, cool location. Storage under refrigeration (2° C) is recommended. Maximum shelf life is six months. (If long term studies are involved, storing the diet at -20° C or colder may prolong shelf life.) Be certain to keep in air tight containers.

*Product Forms Available**	*Catalog #*
1/2" Pellet	1813901

*Other Forms Available On Request

INGREDIENTS

Dehulled Soybean Meal, Maltodextrin, Ground Wheat, Ground Corn, Fish Meal, FOS/Inulin Mixture, Soybean Oil, Wheat Middlings, Calcium Carbonate, Brewers Dried Yeast, Dicalcium Phosphate, Salt, DL-Methionine, Choline Chloride, L-Lysine, Thiamin Mononitrate, Pyridoxine Hydrochloride, Silicon Dioxide, Vitamin A Acetate, Menadione Dimethylpyrimidinol Bisulfite (Vitamin K), Magnesium Oxide, Ferrous Sulfate, Mineral Premix, Cholecalciferol (Vitamin D-3), Biotin, Calcium Pantothenate, DL-Alpha Tocopheryl Acetate, Folic Acid, Riboflavin, Vitamin B-12, Manganese Oxide, Nicotinic Acid, Zinc Oxide.

NUTRITIONAL PROFILE [1]

Nutrient	Value
Protein, %	***23.0***
Arginine, %	1.48
Histidine, %	0.54
Isoleucine, %	1.15
Leucine, %	1.75
Lysine, %	1.51
Methionine, %	0.70
Cystine, %	0.29
Phenylalanine, %	1.04
Tyrosine, %	0.65
Threonine, %	0.89
Tryptophan, %	0.30
Valine, %	1.18
Alanine, %	1.28
Aspartic Acid, %	2.70
Glutamic Acid, %	4.70
Glycine, %	1.19
Proline, %	1.45
Serine, %	1.22
Taurine, %	0.03
Fat (ether extract), %	***5.8***
Fat (acid hydrolysis), %	***6.5***
Cholesterol, ppm	265
Linoleic Acid, %	2.57
Linolenic Acid, %	0.36
Arachidonic Acid, %	0.01
Omega-3 Fatty Acids, %	0.48
Total Saturated Fatty Acids, %	1.14
Total Monounsaturated Fatty Acids, %	1.21
Polyunsaturated Fatty Acids, %	2.90
Fiber (max), %	***8.0***
Neutral Detergent Fiber[2], %	6.8
Acid Detergent Fiber[3], %	2.6
Nitrogen-Free Extract (by difference), %	***47.5***
Starch, %	37.23
Glucose, %	0.23
Fructose, %	0.07
Sucrose, %	1.06
Lactose, %	0.00
Total Digestible Nutrients, %	**59.8**
Energy (kcal/g) [4]	**3.34**

From:	kcal	%
Protein	0.920	27.5
Fat (ether extract)	0.522	15.6
Carbohydrates	1.898	56.8

Minerals	
Ash, %	**5.7**
Calcium, %	1.17
Phosphorus, %	0.69
Phosphorus (available), %	0.46
Potassium, %	0.80
Magnesium, %	0.18
Sulfur, %	0.27
Sodium, %	0.28
Chloride, %	0.49
Fluorine, ppm	22.0
Iron, ppm	348
Zinc, ppm	109
Manganese, ppm	122
Copper, ppm	14
Cobalt, ppm	0.35
Iodine, ppm	0.99
Chromium, ppm	0.94
Selenium, ppm	0.36

Vitamins	
Carotene, ppm	0.1
Vitamin A, IU/g	30
Vitamin D-3 (added), IU/g	2.2
Vitamin E, IU/kg	74
Vitamin K (as menadione), ppm	1.6
Thiamin Hydrochloride, ppm	90
Riboflavin, ppm	15.0
Niacin, ppm	80
Pantothenic Acid, ppm	29
Folic Acid, ppm	2.8
Pyridoxine, ppm	8.01
Biotin, ppm	0.3
Vitamin B-12, mcg/kg	74
Choline Chloride, ppm	2,000
Ascorbic Acid, ppm	0

1. Based on the latest ingredient analysis information. Since nutrient composition of natural ingredients varies, analysis will differ accordingly. Nutrients expressed as percent of ration on an As-Fed basis except where otherwise indicated. Moisture content is assumed to be 10.0% for the purpose of calculations.
2. NDF = approximately cellulose, hemi-cellulose and lignin.
3. ADF = approximately cellulose and lignin.
4. Energy (kcal/gm) - Sum of decimal fractions of protein, fat and carbohydrate x 4,9,4 kcal/gm respectively.

FEEDING DIRECTIONS

Feed ad libitum. Plenty of fresh, clean water should be available at all times.

CAUTION:
Perishable - store upon receipt.
For laboratory animal use only; not for human consumption.

10/1/2009

ISO 9001:2000 CERTIFIED

TestDiet
www.testdiet.com

Butyrate-Fortified Diet (5AVC)

TestDiet® 5SRZ w/6% Tributyrin — 5AVC

DESCRIPTION

[illegible]

NUTRITIONAL PROFILE [1]

Nutrient	Value
[illegible]	***22.9***
[illegible]	1.48
[illegible]	0.54
[illegible]	1.15
[illegible]	1.75
[illegible]	1.51
[illegible]	0.70
[illegible]	0.29
[illegible]	1.04
[illegible]	0.65
[illegible]	0.89
[illegible]	0.30
[illegible]	1.18
[illegible]	1.28
[illegible]	2.70
[illegible]	4.70
[illegible]	1.19
[illegible]	1.45
[illegible]	1.22
[illegible]	0.03
[illegible]	***5.8***
[illegible]	***6.5***
[illegible]	265
[illegible]	2.57
[illegible]	0.36
[illegible]	0.01
[illegible]	0.48
[illegible]	1.14
[illegible]	1.21
[illegible]	2.90
[illegible]	***2.9***
[illegible]	[illegible]
[illegible]	2.6
[illegible]	***53.5***
[illegible]	36.83
[illegible]	0.23
[illegible]	0.07
[illegible]	1.06
[illegible]	0.00
[illegible]	59.8
[illegible]	3.58

[illegible]	[illegible]	[illegible]
[illegible]	0918	25.6
[illegible]	0522	14.6
[illegible]	2141	59.8

[illegible]	
[illegible]	5.7
[illegible]	1.17
[illegible]	0.69
[illegible]	0.46
[illegible]	0.80
[illegible]	0.18
[illegible]	0.27
[illegible]	0.28
[illegible]	0.49
[illegible]	22.0
[illegible]	349
[illegible]	109
[illegible]	122
[illegible]	14
[illegible]	0.35
[illegible]	0.99
[illegible]	0.94
[illegible]	0.36

[illegible]	
[illegible]	0.1
[illegible]	30
[illegible]	2.2
[illegible]	74
[illegible]	1.6
[illegible]	90
[illegible]	15.0
[illegible]	80
[illegible]	29
[illegible]	2.8
[illegible]	8.01
[illegible]	0.3
[illegible]	74
[illegible]	2,000
[illegible]	0

[illegible]

FEEDING DIRECTIONS

[illegible]

[illegible]

TestDiet

Supplementary Figure 3. Formulations of the 3 diets provided to gnotobiotic mice in these experiments. Total fiber levels are enclosed by boxes. For the 5AVC diet (right), tributyrin was provided at the same concentration (6%) as fructo-oligosaccharides/inulin in the high-fiber diet (5SVL, middle) and was otherwise identical and calorically matched. The 5AVC diet was fortified with tributyrin instead of butyrate because butyrate is absorbed in the upper GI tract. Tributyrin is a triacylglycerol that consists of 3 butyrate molecules tethered together *via* a glycerol linkage and is more stable than butyrate. It was used because it is not completely hydrolyzed and absorbed in the upper GI tract and significant levels make it to the colon where it is converted to butyrate in the colon. This has been documented by our group and others (for example, see Donohoe et al. *PLoS ONE* paper cited in main part of this paper). Additional information on each diet is available from Test Diet, and all 3 diets are commercially available from Test Diet.

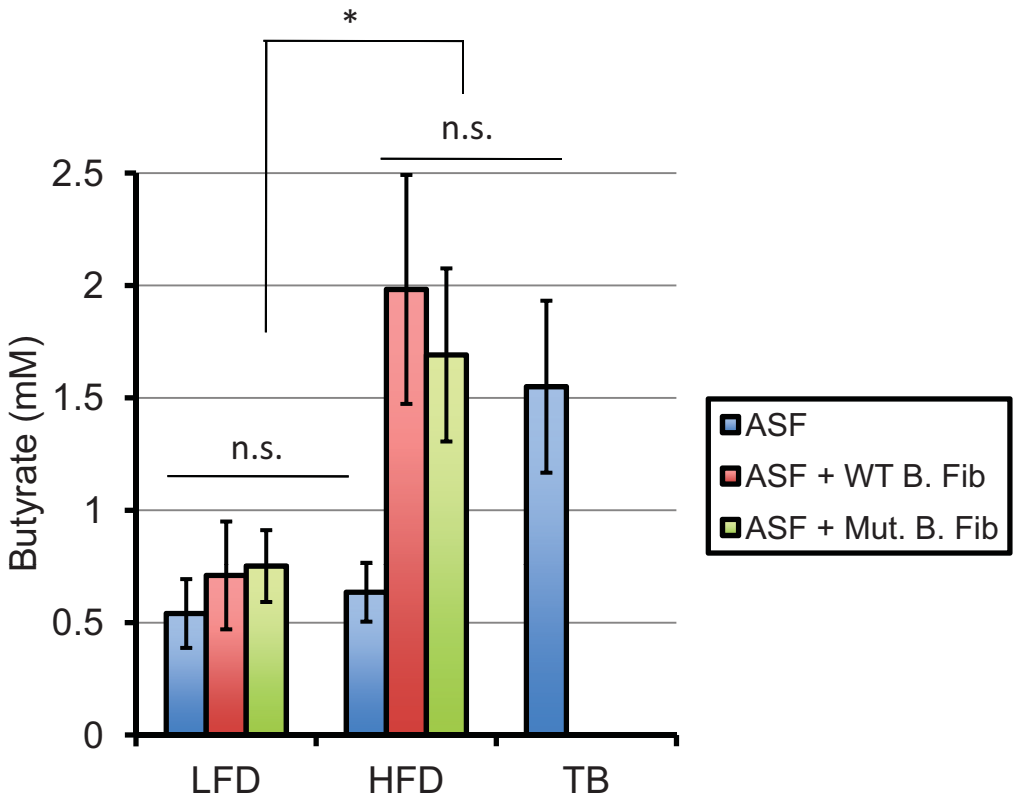

Supplementary Figure 4. A combination of a high-fiber diet and a butyrate-producing bacterium (*Butyrivibrio fibrisolvens)* yields higher levels of butyrate in the lumen of the colon than either factor in isolation. Measurements of luminal contents from the most proximal third of colons were made by LC-MS and included 4 biological replicates for each category. Each histogram shows the mean $\pm$ SE with statistically-significant differences indicated (* $p < 0.05$). ASF, 4 altered Schaedler flora; B. Fib, wild-type (WT) and mutant (Mut) *Butyrivibrio fibrisolvens*; LFD, low-fiber diet; HFD, high-fiber diet; TB, tributyrin-fortified diet.

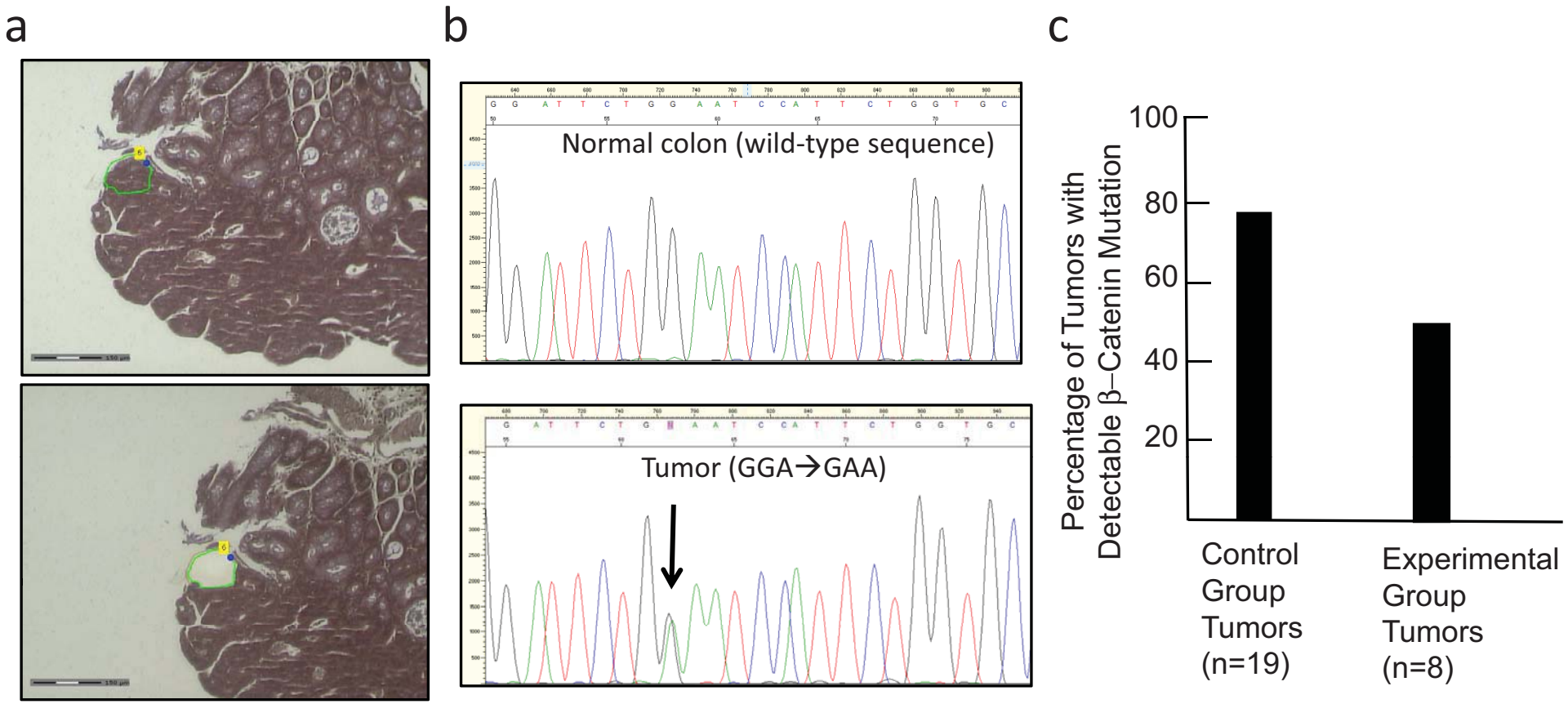

Supplementary Figure 5. Detection of β-catenin mutations in tumor cells. **(a)** Hematoxylin-stained slide before (top) and after (bottom) laser-capture microdissection to document the isolation of tumor cells. The region of interest is highlighted by a green circle. **(b)** Representative DNA sequence chromatograms showing a segment of β catenin from normal colonic tissue (top) and a laser-captured tumor sample (bottom) with a heterozygous point mutation (GGA-to-GAA) at codon 34, which results in a Gly-to-Glu substitution (G34E). **(c)** Percentage of tumors with a detectable mutation of β catenin in a mutational hotspot region that includes codons 32-41. The experimental group tumors were from mice colonized with ASF plus WT *B. fibrisolvens* and that were also provided a high-fiber diet.

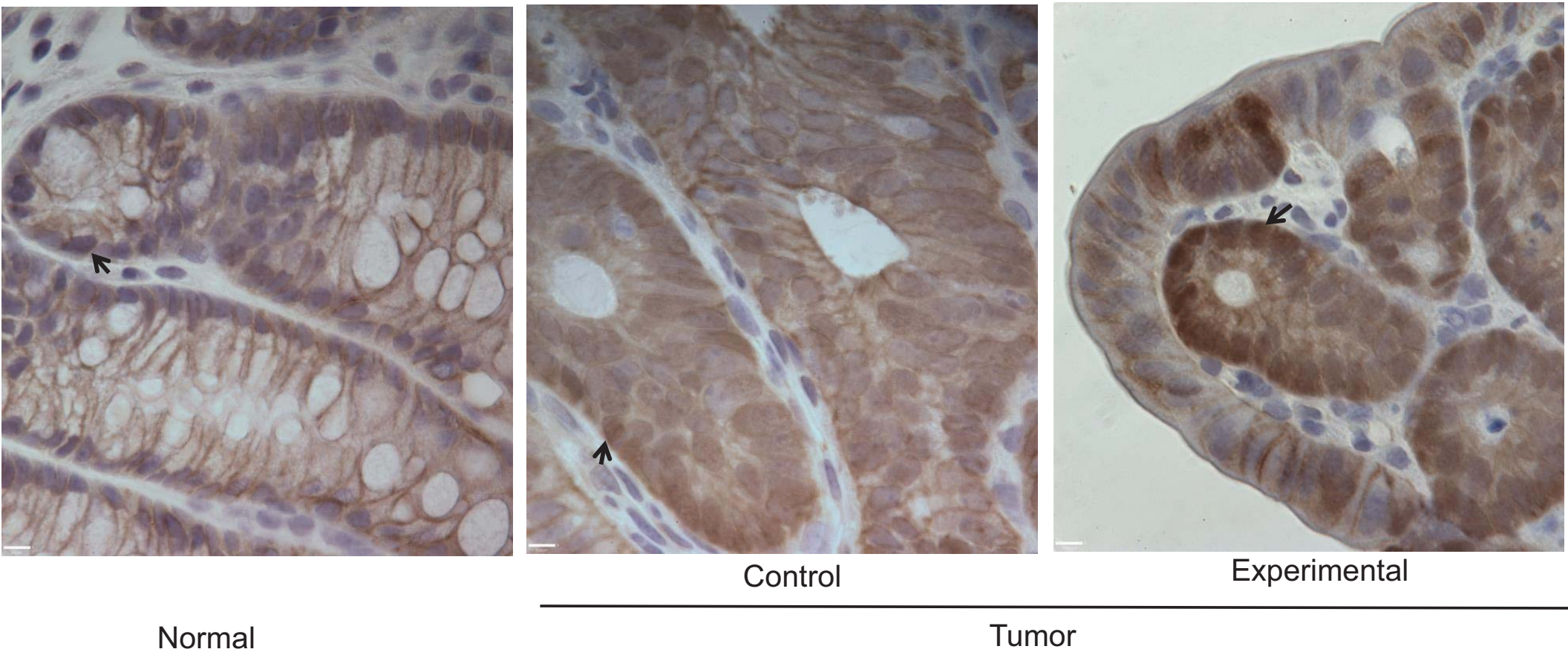

Supplementary Figure 6. Analysis of β catenin nuclear localization in control and experimental tumors. Representative IHC images of β-catenin in normal colonic tissue (left panel) and colorectal tumors from control (middle panel) and experimental (right panel) groups. Arrows point to examples of nuclei that are negative (normal) or positive (tumors) for β-catenin. Experimental tumors were from mice colonized with ASF plus WT *B. fibrisolvens* and that were also provided a high-fiber diet. 10 tumors were analyzed per group.

a

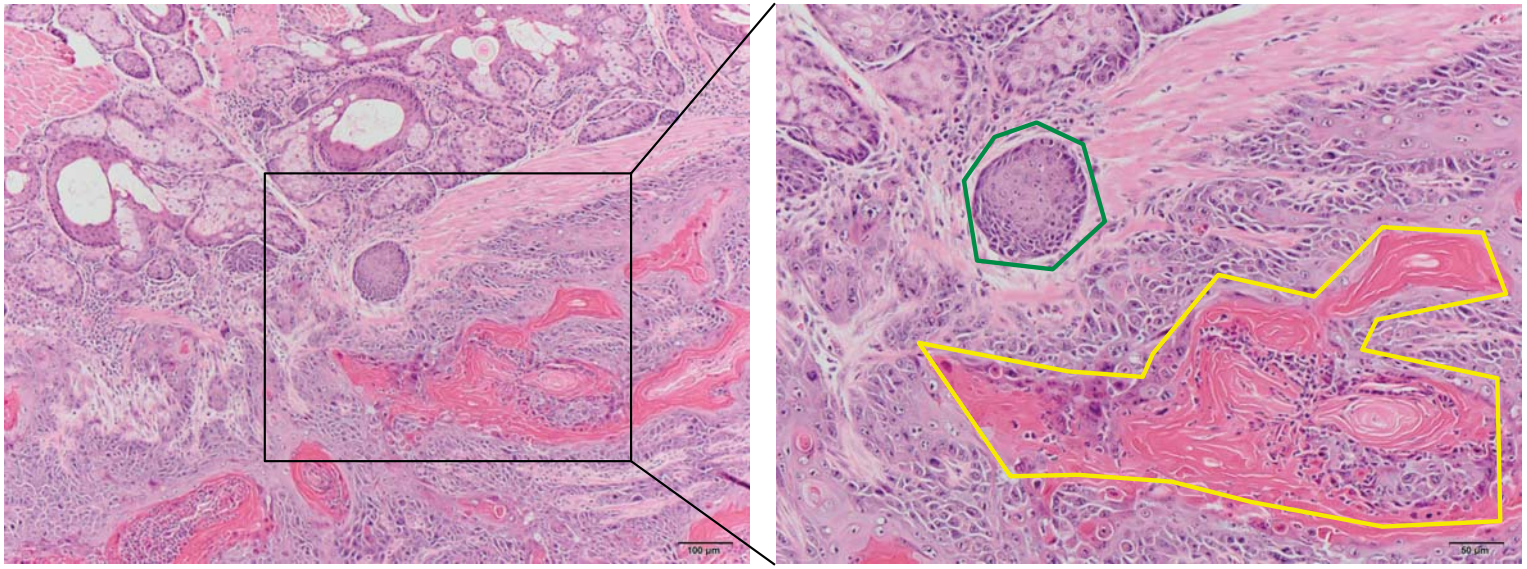

b

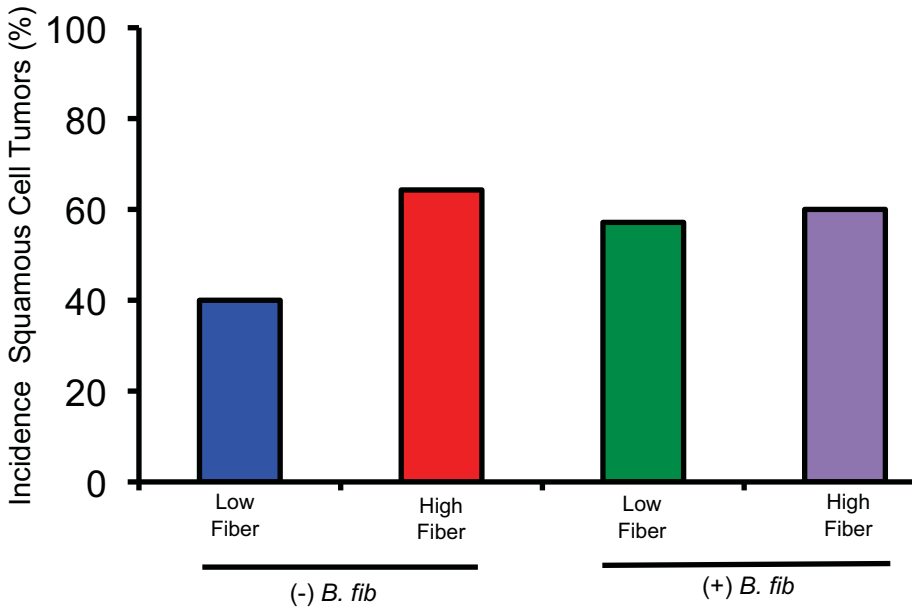

Supplementary Figure 7. Characterization of squamous cell tumors. **(a)** Representative image of H&E-stained tumor section at lower (left) and higher (right) magnifications. Maturation of neoplastic cells (circled in green) and production of keratin by these cells (outlined in yellow) are two hallmarks of squamous cell tumors. Scale bars are shown at bottom right. **(b)** Incidence of squamous cell tumors in mice from different treatment groups following 5 AOM/3 DSS dose regimen.

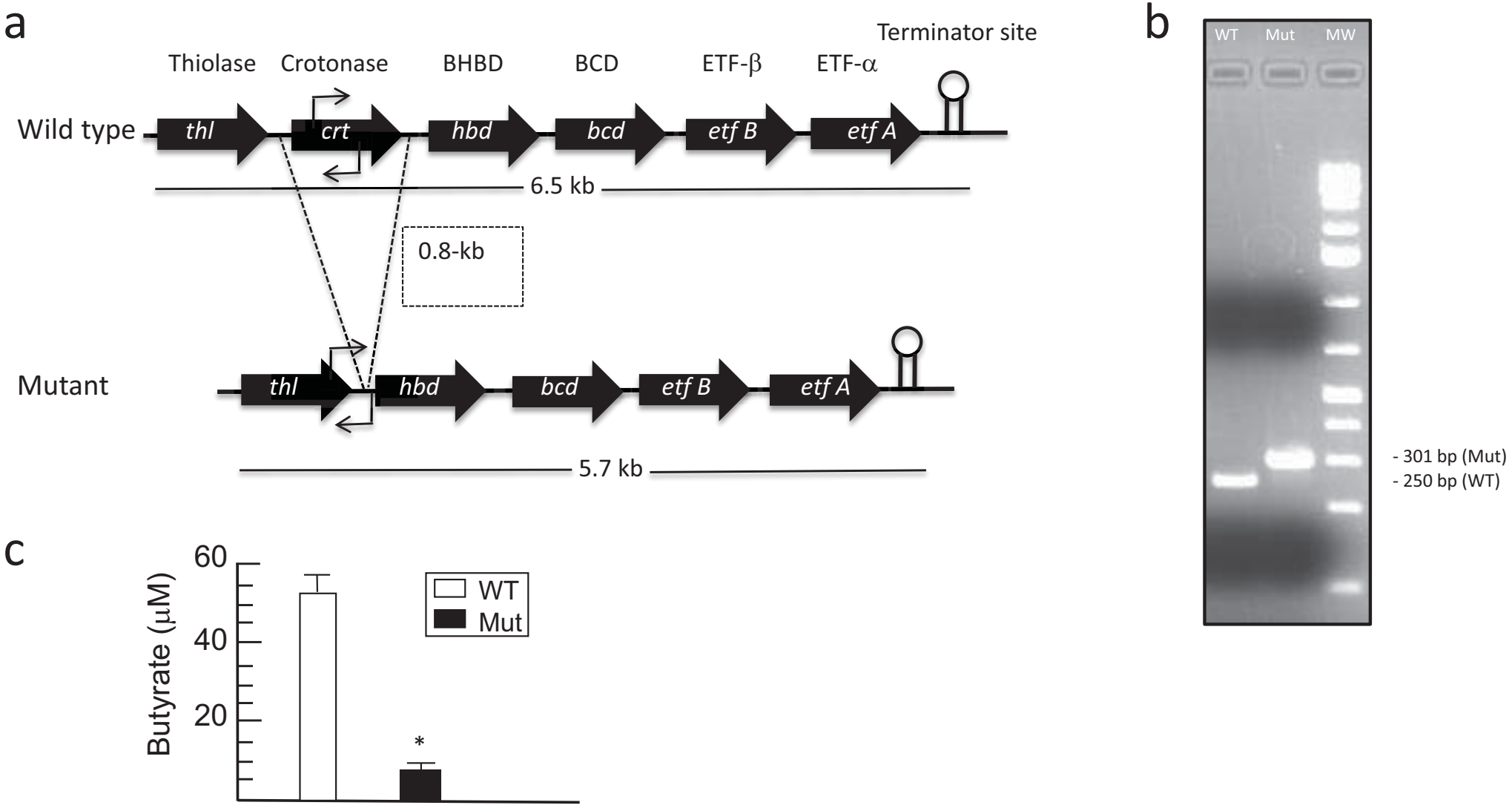

Supplementary Figure 8. Analysis of wild-type and mutant *B. fibrisolvens* strains. **(a)** Schematic of the butyryl-CoA synthesis operon in the wild-type and mutant strains. Adapted from a previous publication[15]. The dotted line shows the position of the 0.8-kb deletion that ablates the *crt* gene in the mutant. The position of primer pairs that amplify PCR products specific to the wild-type and mutant strains are shown. **(b)** Confirmation of the wild-type (WT) and mutant (Mut) *B. fibrisolvens* strains by PCR using primers shown in panel a. MW, 1-Kb Plus molecular-weight ladder. PCR product sizes are shown on the right. (**c**) LC-MS measurements of butyrate concentrations from media of wild-type (WT) and mutant (Mut) strains grown in ASF media supplemented with FOS/inulin under anaerobic conditions. Results are from 3 independent experiments and are presented as mean $\pm$ SE with significant differences noted (*, $p < 0.01$).

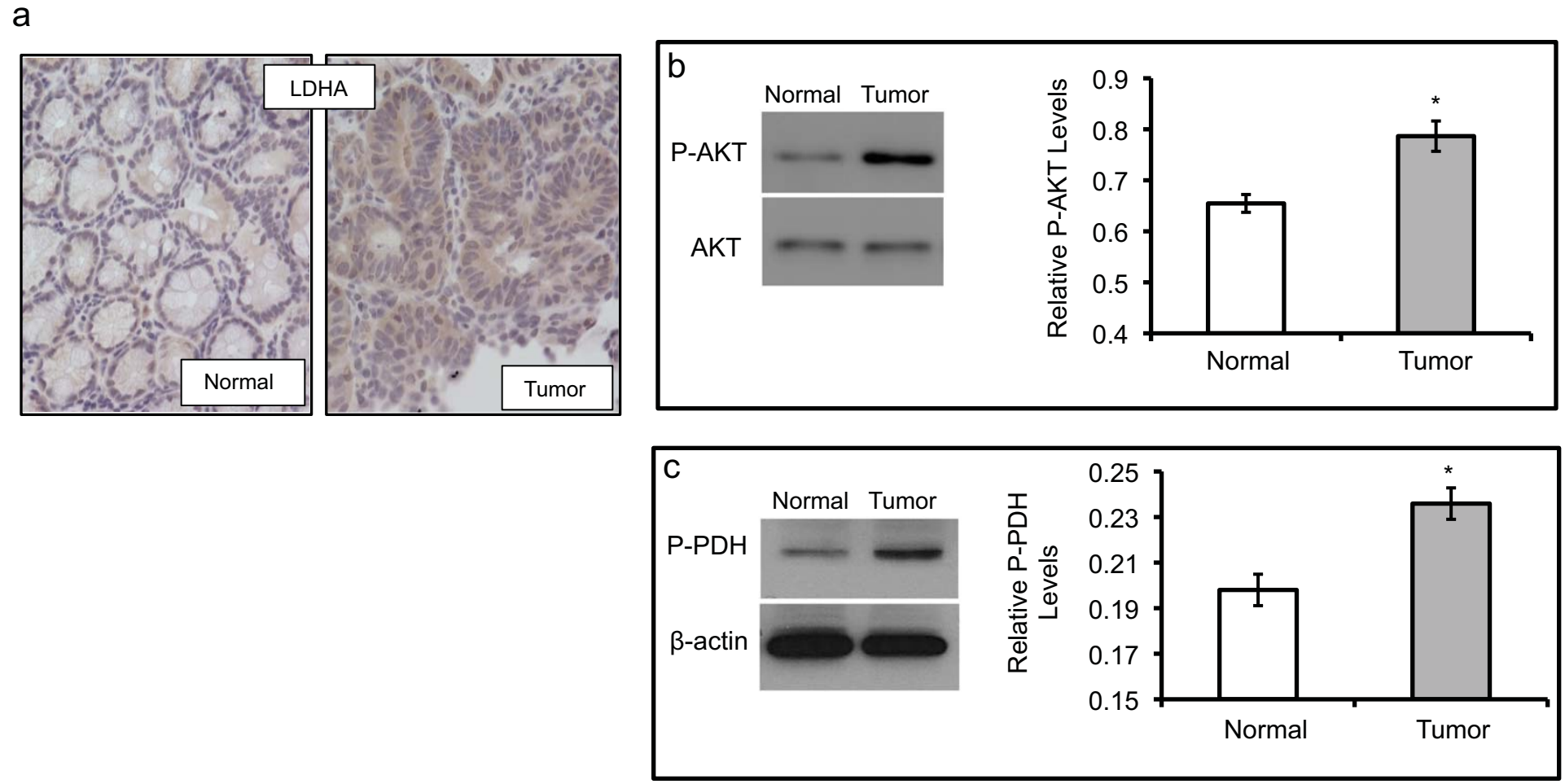

Supplementary Figure 9. Expression of Warburg effect markers. **(a)** Representative IHC of LDHA in normal colonic tissue and colorectal tumor. **(b, c)** Western blot analysis of P-AKT (Ser473) **(b)** and P-PDH (Ser293) **(c)** levels in normal colonic tissues and colorectal tumors. Total AKT and β-actin served as loading controls. Left, each image is representative of 3 independent experiments. Right, each histogram shows the mean ± SE with significant differences indicated (*$p<0.05$) based on 3 independent experiments.

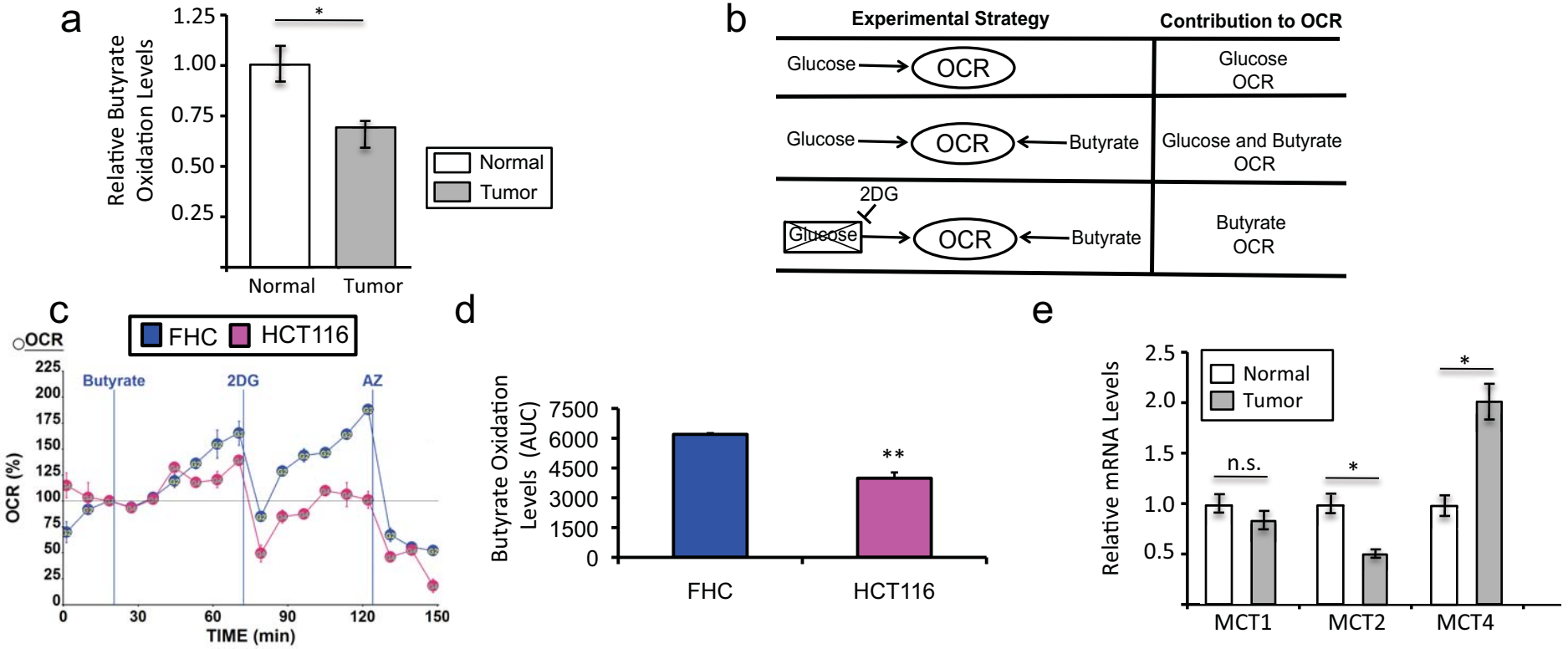

Supplementary Figure 10. Butyrate oxidation and uptake in colorectal tumors and normal colonic tissues. **(a)** Butyrate oxidation in tissues from gnotobiotic mouse model based on flux experiments where ^{13}C-butyrate was added to cells and ^{13}C-CO2 levels were then measured by isotope-ratio mass spectrometry. Each histogram shows the mean ± SE with significant differences indicated (*p < 0.05) for 4-6 independent experiments. **(b-d)** Butyrate oxidation in noncancerous fetal human colonocytes (FHC) and HCT116 colon cancer cells based on Seahorse flux experiments. **(b)** Diagram showing experimental strategy used to measure butyrate oxidation in cells over time with Seahorse Analyzer. Assays were initiated in a KHB buffer where glucose (2.5 mM final) is the only exogenous substrate for oxidative phosphorylation (top). After 20 minutes, butyrate (5 mM final) is added (middle). Injection of 2-deoxyglucose (2DG) at the 70-minute time point inhibits glucose oxidation leaving butyrate as the major oxidative substrate (bottom). **(c)** Oxygen consumption rates (OCR) for FHC and HCT116 cells relative to basal levels (glucose only) at time point 0. Time points for butyrate, 2DG, and sodium azide (AZ) injection are indicated by vertical lines. AZ inhibits oxidative phosphorylation to end the assay. Data points represent the average OCR (%) over 3-5 replicates per experimental condition. FHC and HCT116 cells were assayed together in the same experimental run and cell numbers were kept identical between the two cell lines. **(d)** Butyrate oxidation levels as measured by average area under the curve (AUC) between 2DG and AZ treatments as shown in panel c. Each histogram is based on 10-15 measurements and shows the mean ± SE with significant differences indicated (**p < 0.01). **(e)** Relative mRNA levels of monocarboylate transporter (MCT) genes normalized to *Gapdh* levels in normal colonic tissue and tumors based on RT-qPCR experiments. Each histogram shows the mean ± SE with significant differences indicated (* p < 0.05; n.s., not significant) for 3-6 independent experiments.

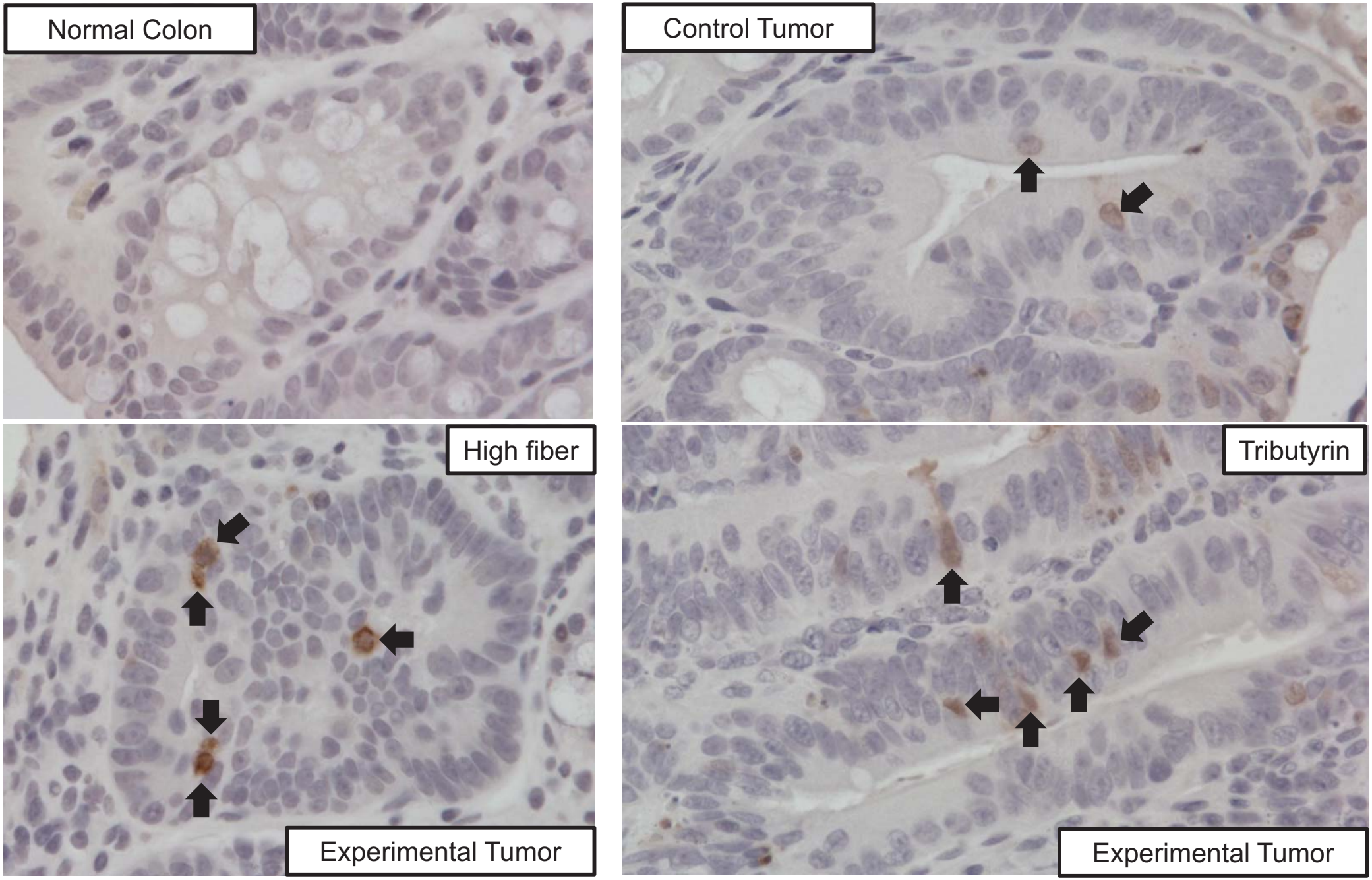

Supplementary Figure 11. Representative IHC images showing cleaved caspase 3 positive cells (arrows) in normal colonic tissue and tumors from mice in control and experimental conditions.

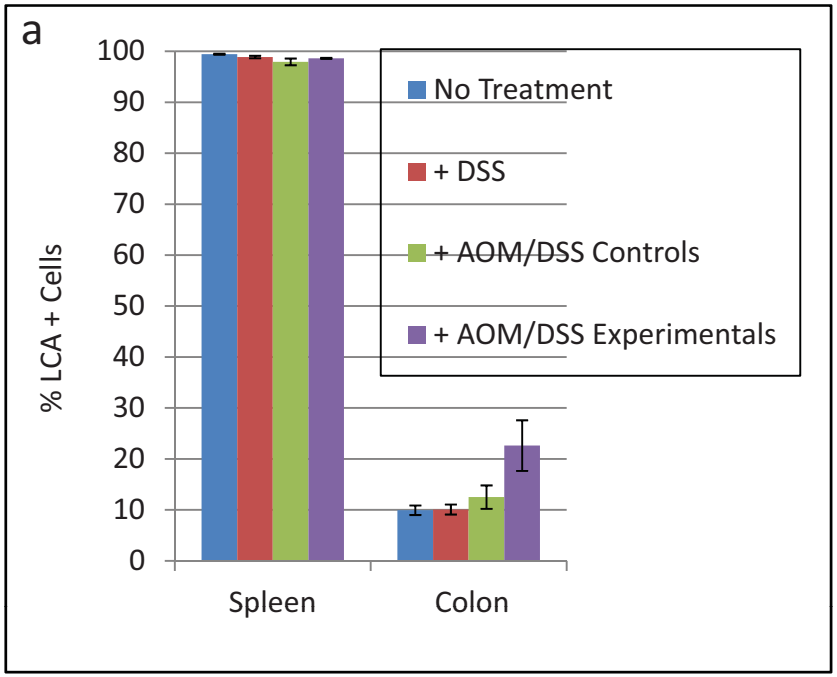

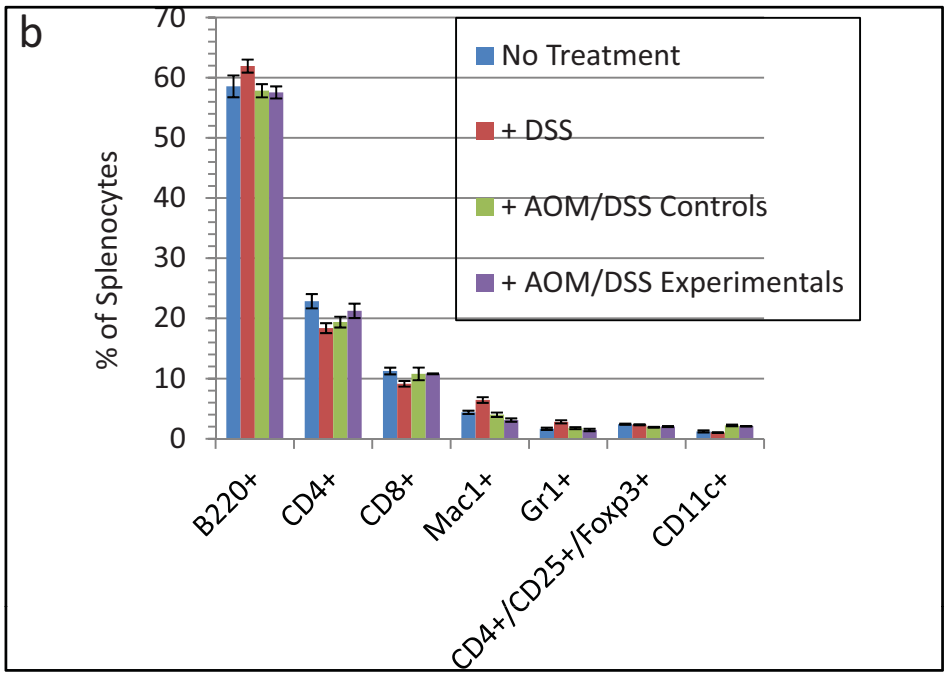

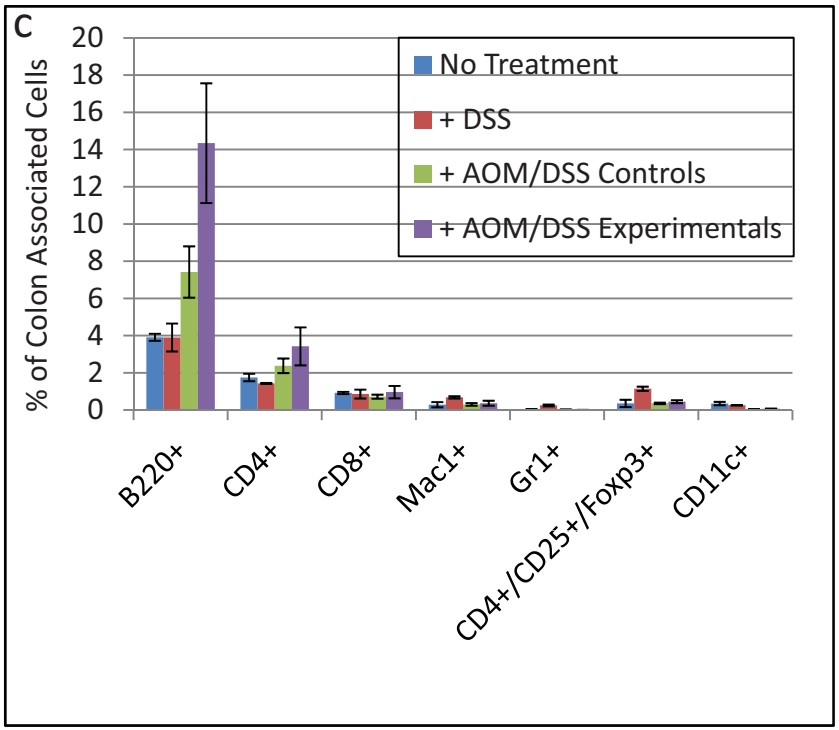

Supplementary Figure 12. Flow cytometric analysis of immune cell populations from BALB/c mice colonized with the 4 ASF and *B. fibrisolvens* in gnotobiotic isolators. The key within each panel indicates which mice were untreated (to represent basal conditions), treated with DSS only (mice were analyzed on the last day of the second 5-day cycle to represent an acute inflammatory stimulus) or treated with AOM/DSS (mice were analyzed 2.5 months after being treated with AOM following a 1 AOM/2 DSS regimen to represent inflammation associated with tumourigenesis). For AOM/DSS, control and experimental groups were analyzed separately as indicated. Histograms show means ± SE, and 4-8 mice were analyzed for each of the 4 groups of mice in panels a-e. **(a)** Relative abundance of hematopoietic cells in spleens and colons based on cell-surface expression of LCA (leukocyte common antigen). **(b-c)** Relative abundance of specific hematopoietic lineages in spleen (b) and colon (c). B220, B cells; CD4+, T helper (Th) cells; CD8+, cytotoxic T cells; Mac1+, macrophages; Gr1+, granulocytes; CD4+/CD25+/Foxp3+, regulatory T cells (Tregs).

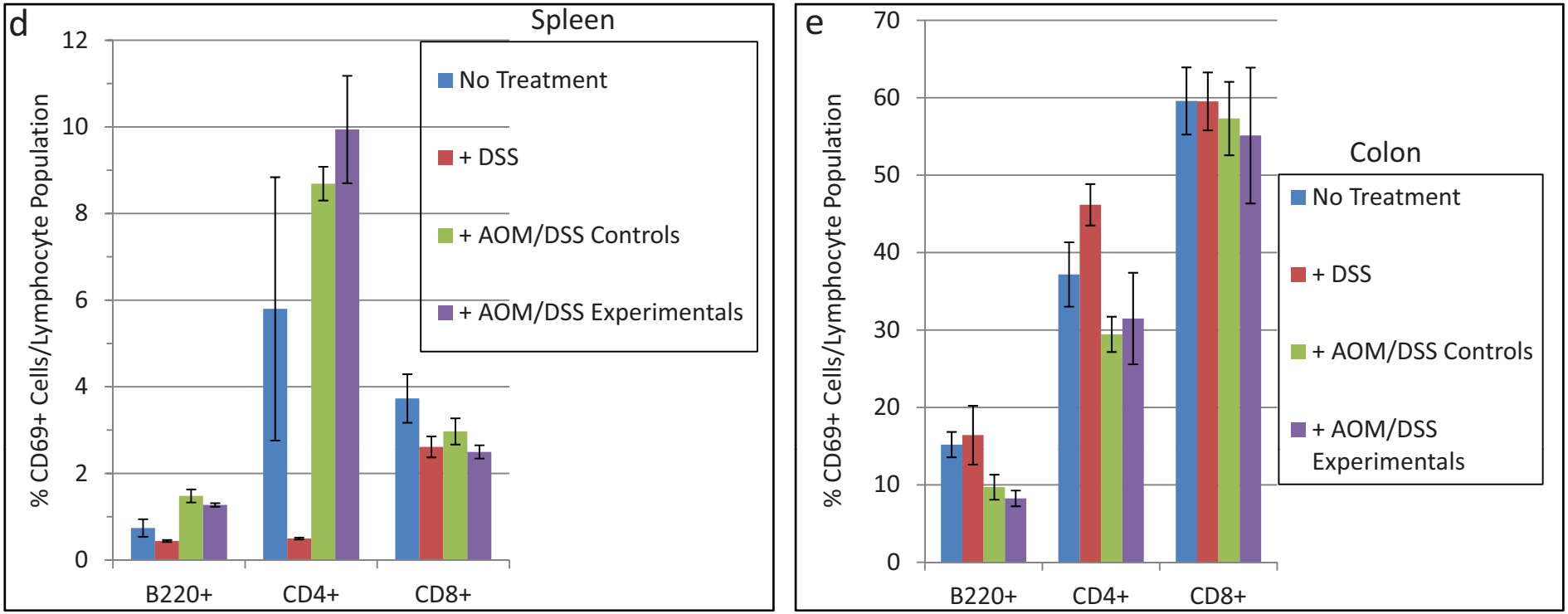

Supplementary Figure 12 (continued). (d-e) Percentage of lymphocytes that express the CD69 activation marker in spleens (d) and colons (e).

Overall, these results indicate that the abundance of immune cells in the colon is relatively low in the gnotobiotic model even when they are treated with DSS or AOM/DSS (a). SPF mice treated with DSS have been shown to have a much greater induction of immune cell populations in the colon[16-21] (PMIDs: 20467900, 23012474, 21815907, 21498668, 22089030, 18381351). This supports the idea that the 4 ASF bacteria and *B. fibrisolvens* are unable to induce a strong inflammatory response compared to the diverse microbiota in conventional, SPF mice. The slight elevation in immune cells in the colon of AOM/DSS experimentals (colonized with *B. fibrisolvens* and provided a HFD) (a) is compatible with a slight increase in crypt abscesses undergoing apoptosis in this same group of mice based on H&E analyses (Supplementary Figure 12). In addition, the lymphocyte populations in the colon are not activated to a greater extent based on CD69 status (e), and this is consistent with cytokine levels not being elevated (Supplementary Figures 11). Finally, even in response to DSS treatment, bloody stool and rectal prolapses were not observed in the gnotobiotic mice (data not shown), which occurs in conventional SPF mice treated with DSS and is an overt, external sign of colonic inflammation.

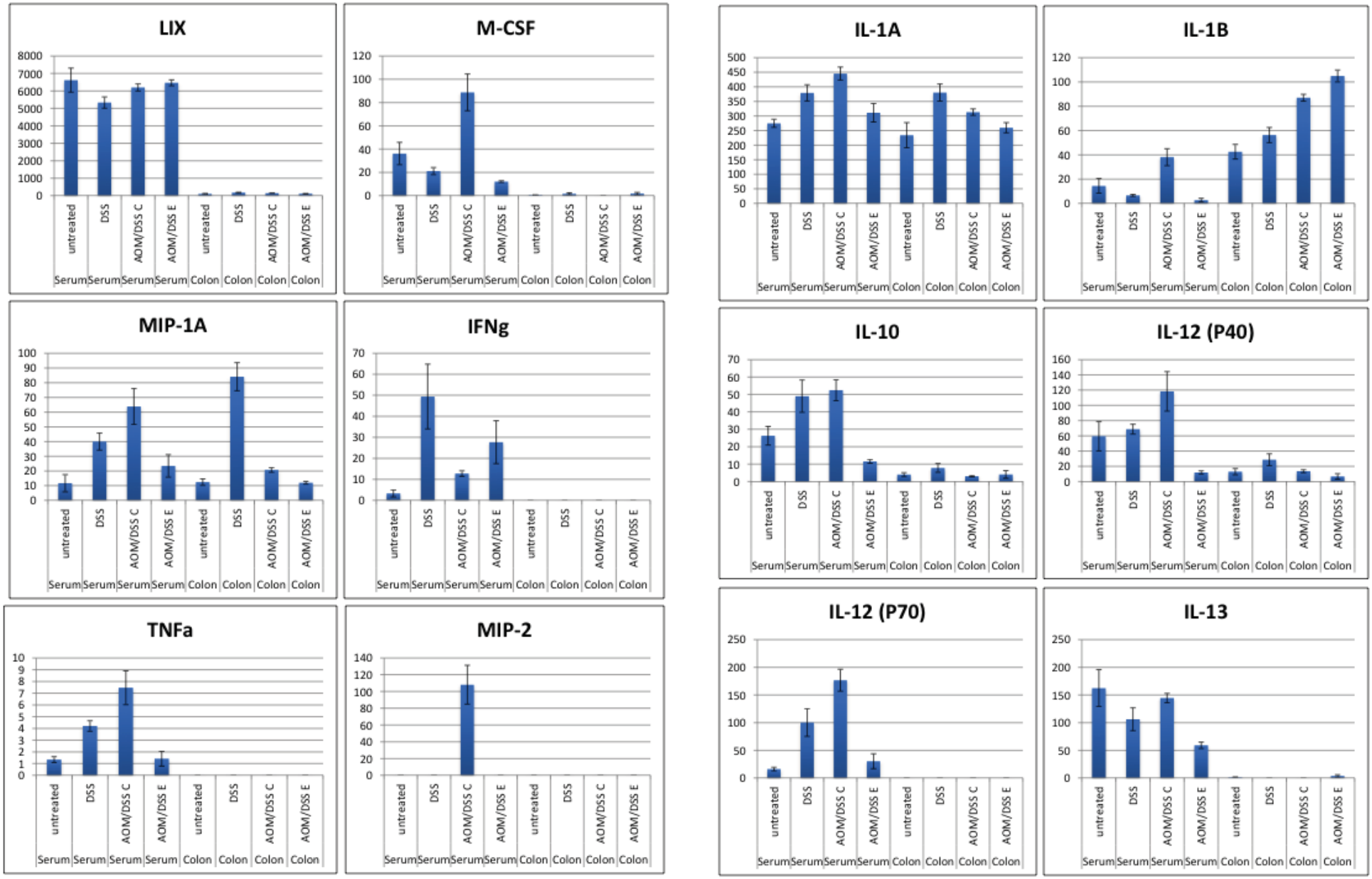

Supplementary Figure 13. Serum and colonic cytokine levels (pg/mL) from BALB/c mice colonized with the 4 ASF and *B. fibrisolvens* in gnotobiotic isolators based on Luminex assays. Mice were untreated (to represent basal conditions), treated with DSS only (mice were analyzed on the last day of the second 5-day cycle to represent an acute inflammatory stimulus) or treated with AOM/DSS (mice were analyzed 2.5 months after being treated with AOM following 1 AOM/2 DSS regimen to represent inflammation associated with tumourigenesis). For AOM/DSS, control (C) and experimental (E) groups were analyzed separately as indicated. Histograms show mean ± SE, and 4-8 mice were analyzed for each of the 4 groups of mice.

Overall, these results indicate that cytokine levels are only modestly affected by DSS or AOM/DSS treatment (compared to untreated) in this gnotobiotic model as compared to previous studies of SPF mouse models (PMID: 22665990). These data also support the idea that the observed difference in tumorigenesis between the experimental and control groups is not due to differences in inflammation. For example, there are very few differences between colonic C and E values, and the few observed differences are subtle with different directionalities (and the opposing directionalities do not correspond to differences in pro-inflammatory versus immunosuppressive cytokines). These findings are consistent with the flow cytometry and H&E data (Supplemental Figures 10 and 12, respectively), which also suggest that inflammation is not a significant factor in this gnotobiotic model.

Supplementary Figure 13 Continued

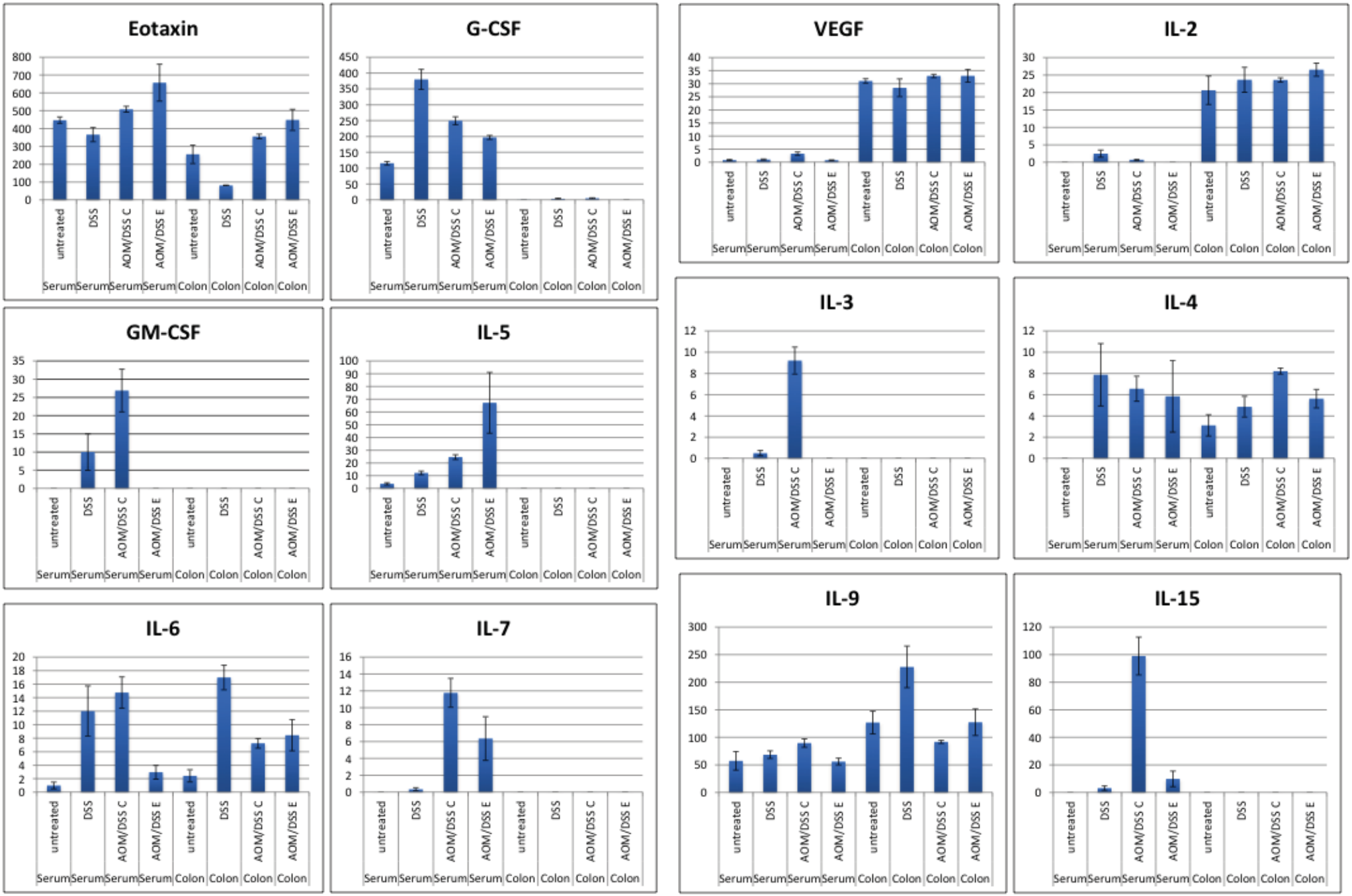

Supplementary Figure 13 Continued

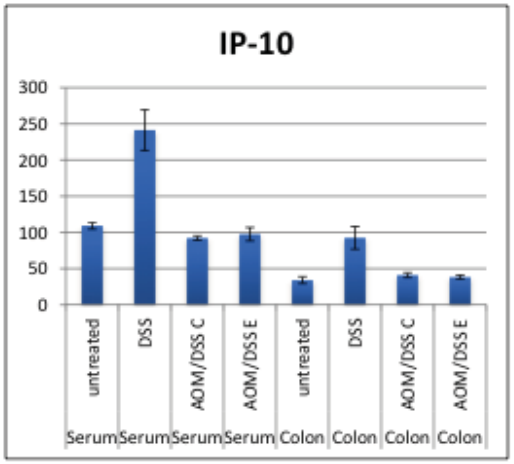

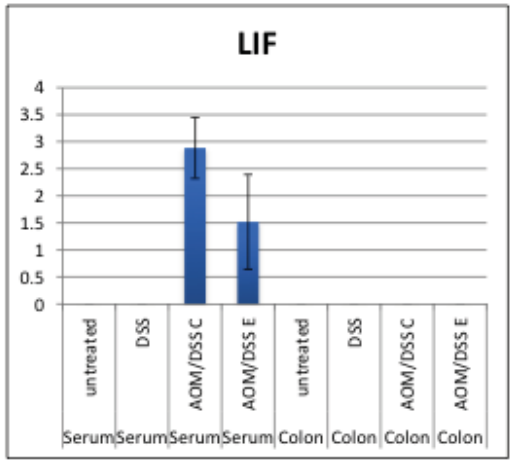

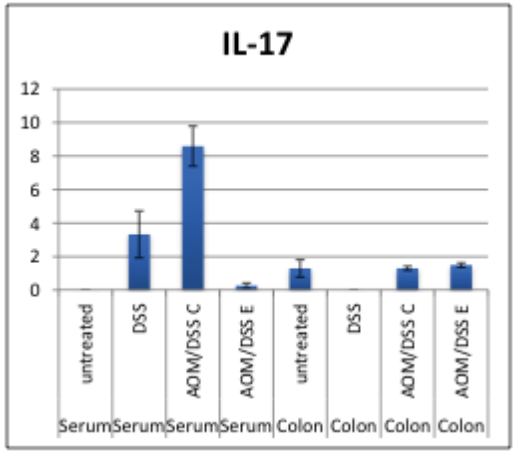

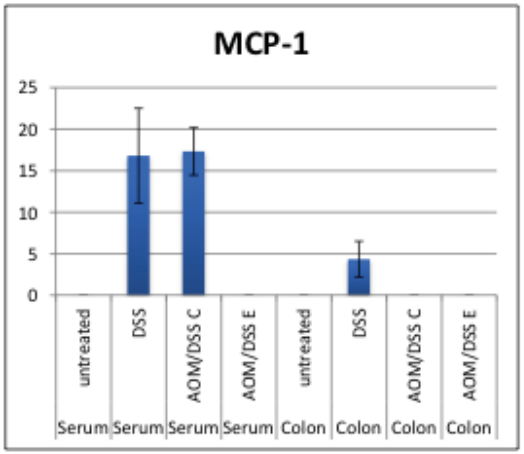

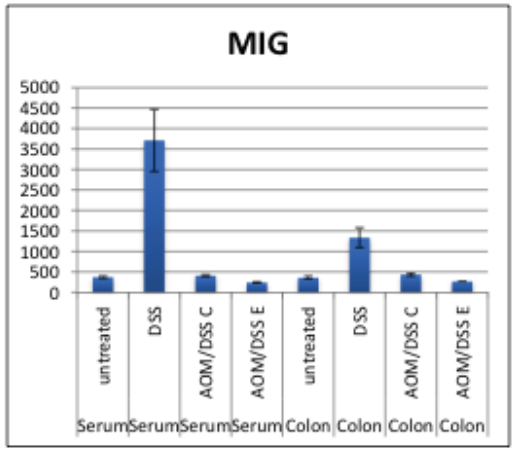

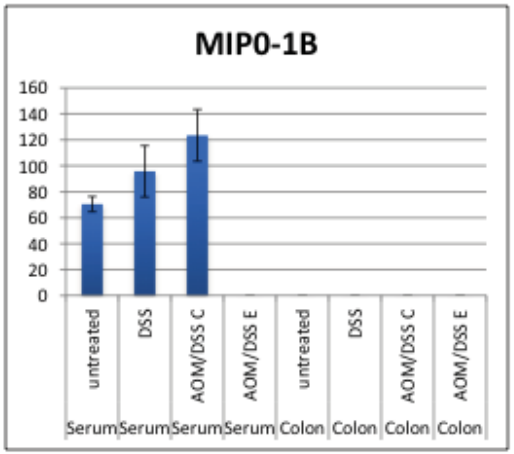

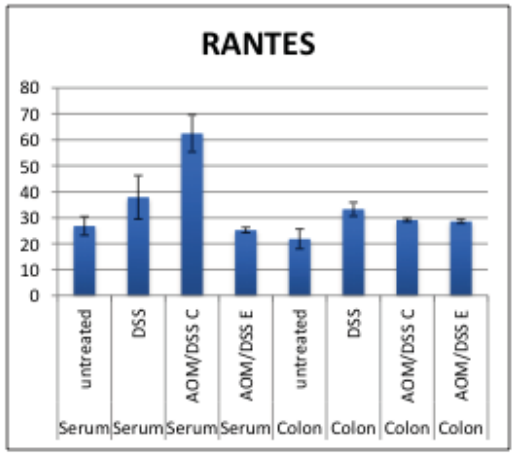

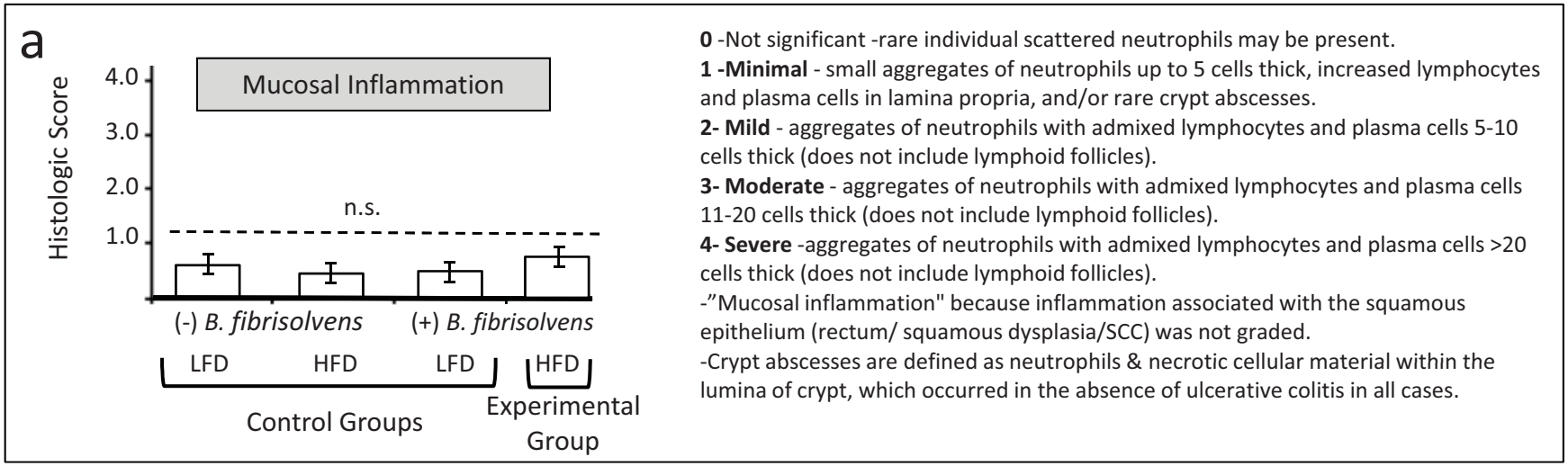

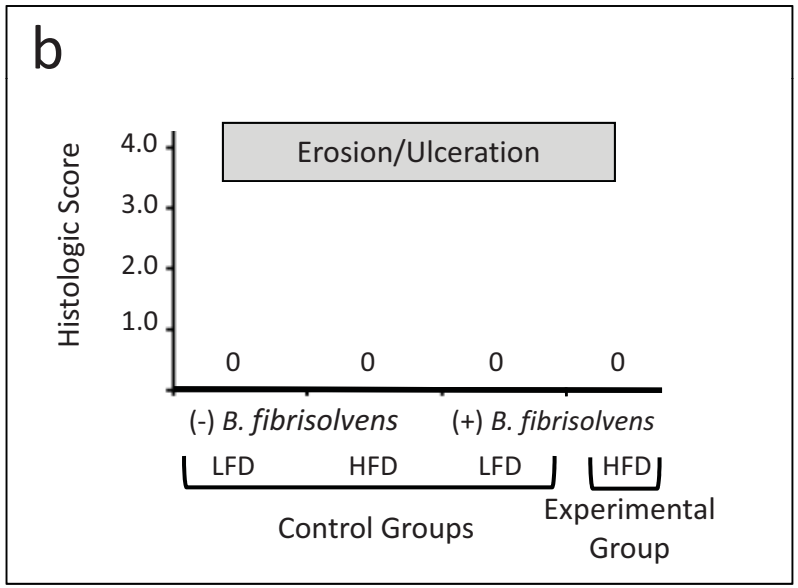

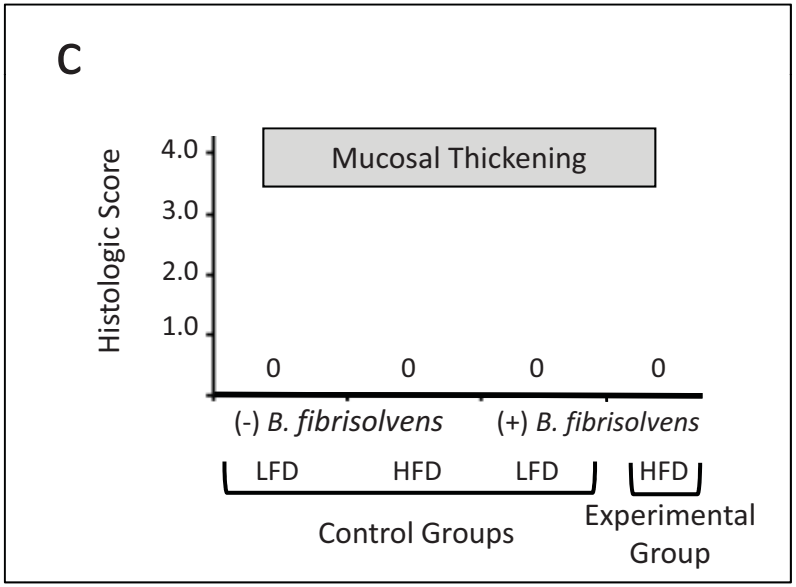

Supplementary Figure 14. Minimal inflammation based on histologic assessment of H&E-stained sections of colorectal tumor sections from 7-10 mice of each treatment group 5 months after exposure to the 5 AOM/3 DSS regimen. **(a)** Mucosal inflammation with key and definitions shown at right. Histograms show the mean ± SE. n.s., not significant. **(b)** Erosion/ulceration values were zero for all 34 specimen in the 4 different treatment groups. Erosion refers to a defect in the mucosa (epithelium, lamina propria, muscularis mucosae) with an underlying tissue reaction. It does not refer to erosion on the top of tumors as this would be likely due to trauma in the colonic lumen due to the bulk of the mass rather than a primary erosive/ulcerative process. Ulceration refers to a defect that penetrates the entire mucosal layer (mucosal epithelium, lamina propria, and muscularis mucosa). **(c)** Mucosal thickening values were zero for all 34 specimen in the 4 different treatment groups. Mucosal thickening refers to enough inflammatory cells infiltrating and aggregating to thicken the mucosa and cause significant increased separation between adjacent crypts. It does not refer to the typical thickening of the mucosa in dysplastic areas of tumors.

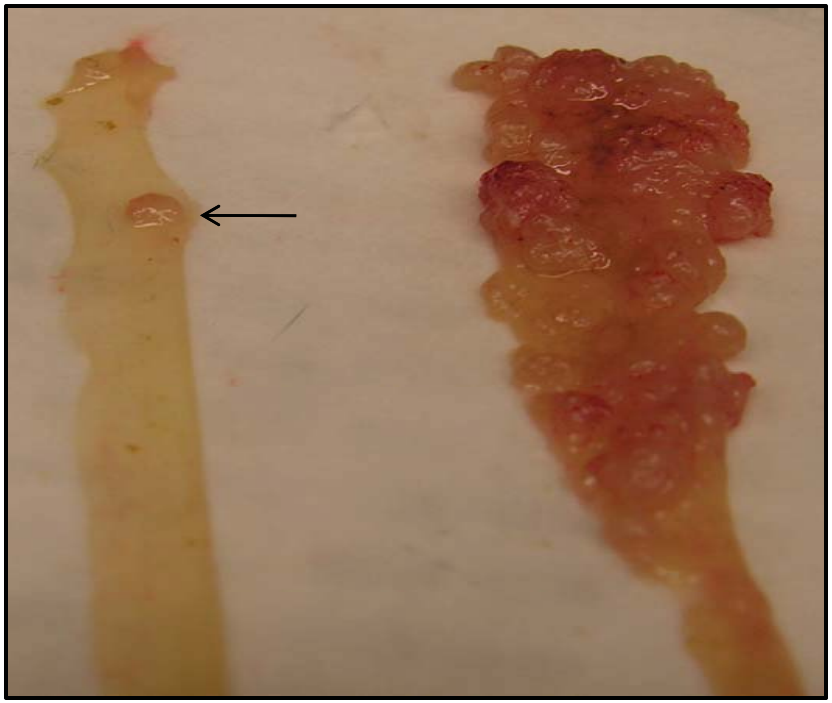

Supplementary Figure 15. Control experiment demonstrating that inflammation plays a minor role in colorectal tumorigenesis in the gnotobiotic model where BALB/c mice were polyassociated with 4 ASF plus *B. fibrisolvens* and then treated with AOM/DSS. **Left,** 1 tumor (arrow) is present in a splayed-open colon from a polyassociated mouse that received 1 AOM/2 DSS while maintained in a gnotobiotic isolator for the entire experiment. **Right,** Many tumors are present in a splayed-open colon from an identical polyassociated mouse that received 1 AOM injection in the same gnotobiotic isolator but was subsequently moved to a specific pathogen free (SPF) facility where it became conventionalized with a complete, albeit undefined, microbiota. This conventionalized mouse received the same 2 DSS regimen and diet in the SPF facility and was necropsied at the same time (5 months after the AOM injection), but exhibited much greater colonic inflammation and a >10X increase in tumor burden. This stark difference was consistently observed in 3 pairs of mice and suggests that the ASF and *B. fibrisolvens* are unable to initiate a robust inflammatory response following DSS treatment, which restricts tumorigenic potential. In contrast, the complete microbiota in conventionalized mice trigger a strong inflammatory response following DSS treatment (which breaks down the barrier function of the gut and brings microbiota from the lumen in close physical proximity with immune cells from the lamina propria) and greatly exacerbates AOM-induced tumorigenesis.

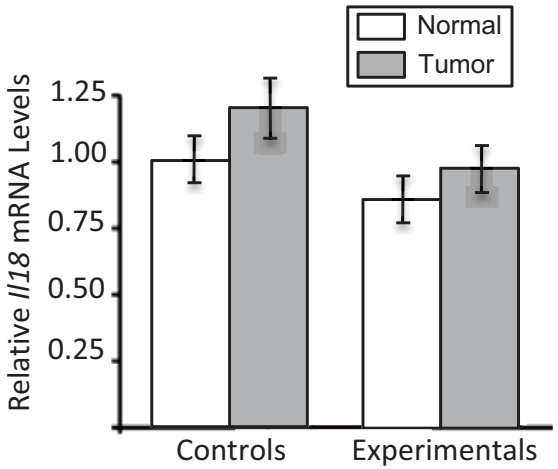

Supplementary Figure 16. Relative *Il18* mRNA levels normalized to *Gapdh* levels in normal colonic tissue and tumors based on RT-qPCR experiments. Each histogram shows the mean ± SE for 3 independent experiments.

Supplementary Table 1. Luminal Concentrations (μM) of Other Two Major SCFAs (Propionate and Acetate)				
Microbiota (4 ASF ± *B. fib*):	(-) *B. fibrisolvens*		(+) *B. fibrisolvens*	
Diet:	Low fiber	High fiber	Low fiber	High fiber
Propionate	963 ± 63	3433.4 ± 2427.8	3290.2 ± 2326.5	2400 ± 400.1
Acetate	7326 ± 1494	25668 ± 20529	35541 ± 5247	28199 ± 9180

Numbers refer to mean ± SE based on n = 3 biological replicates (separate animals)

Supplementary Table 2. Clinical Information Regarding Human Adenocarcinomas					
Patient #	Tissue Procurement Facility	Gender	Age	Tumor Stage	Tumor Position*
1	UNC	Female	62	2	
2	UNC	Male	67	2	
3	UNC	Male	83	2	
4	UNC	Female	58	2	
5	UNC	Male	77	2	
6	CSU	Male	67	2	Ascending colon
7	CSU	Male	47	1	Sigmoid colon
8	CSU	Male	86	T3	Ascending colon
9	CSU	Male	74	T3	Sigmoid colon
10	CSU	Female	55	Tis (carcinoma in situ: intraepithelial or invasion of lamina propria)	Sigmoid colon
11	CSU	Male	76	T3	Ascending colon

*Each adenocarcinoma sample had a macroscopically normal mucosal sample that served as a control; the normal samples were 4-6 cm away from the adenocarcinomas for the UNC tissue procurement facility.
*Blank fields are due to information not provided by tissue procurement facility.

Supplementary Table S3. Statistical tests used for each figure panel.

Figure	Outcome	Type	Statistical Test
1A	Tumor Multiplicity	Parametric	ANOVA/Tukey
1B	Tumor Size	Parametric	ANOVA/Tukey
1C	Tumor Grade	Non-parametric	Kruskal-Wallis
2B	Relative LDHA Levels	Parametric	Two-tailed t test
2E	Butyrate Measurements	Parametric	ANOVA/Tukey
2H	Relative H3 Acetylation Levels	Parametric	ANOVA/Tukey
2I	HDAC Activity Levels	Parametric	ANOVA/Tukey
3A,C,E	Relative H3ac Levels	Parametric	ANOVA/Tukey
3B,D,F	Relative mRNA Levels	Parametric	ANOVA/Tukey
3G	Cleaved Caspase-3 Quantification	Non-parametric	Kruskal-Wallis
3H	Relative Ki-67 Levels	Non-parametric	Kruskal-Wallis
4A	Butyrate Measurements	Parametric	Two-tailed t test
4D	Relative H3 Acetylation	Parametric	Two-tailed t test
S4	Butyrate Measurements	Parametric	ANOVA/Tukey
SF8	Butyrate Measurements	Parametric	Two-tailed t test
SF9	Relative P-PDH and P-AKT (WB)	Parametric	Two-tailed t test

SF10a,d	Butyrate Oxidation Measurements	Parametric	Two-tailed t test
SF10E	Relative MCT expression (RT-qPCR)	Parametric	ANOVA/Tukey
SF12	Flow Cytometry Data	Parametric	ANOVA/Tukey
SF14	Histological Scoring	Non-parametric	Kruskal-Wallis
SF16	Relative IL18 expression (RT-qPCR)	Parametric	ANOVA/Tukey

Supplemental References

1 Barcenilla, A. *et al.* Phylogenetic relationships of butyrate-producing bacteria from the human gut. *Applied and environmental microbiology* **66**, 1654-1661 (2000).

2 Pryde, S. E., Duncan, S. H., Hold, G. L., Stewart, C. S. & Flint, H. J. The microbiology of butyrate formation in the human colon. *FEMS microbiology letters* **217**, 133-139 (2002).

3 Rosenberg, D. W., Giardina, C. & Tanaka, T. Mouse models for the study of colon carcinogenesis. *Carcinogenesis* **30**, 183-196, doi:10.1093/carcin/bgn267 (2009).

4 Wostmann, B. S. The germfree animal in nutritional studies. *Annual review of nutrition* **1**, 257-279, doi:10.1146/annurev.nu.01.070181.001353 (1981).

5 Duncan, S. H., Barcenilla, A., Stewart, C. S., Pryde, S. E. & Flint, H. J. Acetate utilization and butyryl coenzyme A (CoA):acetate-CoA transferase in butyrate-producing bacteria from the human large intestine. *Applied and environmental microbiology* **68**, 5186-5190 (2002).

6 Kaiser, S. *et al.* Transcriptional recapitulation and subversion of embryonic colon development by mouse colon tumor models and human colon cancer. *Genome biology* **8**, R131, doi:10.1186/gb-2007-8-7-r131 (2007).

7 Ohkawara, S., Furuya, H., Nagashima, K., Asanuma, N. & Hino, T. Oral administration of butyrivibrio fibrisolvens, a butyrate-producing bacterium, decreases the formation of aberrant crypt foci in the colon and rectum of mice. *The Journal of nutrition* **135**, 2878-2883 (2005).

8 Uronis, J. M. & Threadgill, D. W. Murine models of colorectal cancer. *Mammalian genome : official journal of the International Mammalian Genome Society* **20**, 261-268, doi:10.1007/s00335-009-9186-5 (2009).

9 McIntyre, A., Gibson, P. R. & Young, G. P. Butyrate production from dietary fibre and protection against large bowel cancer in a rat model. *Gut* **34**, 386-391 (1993).

10 Perrin, P. *et al.* Only fibres promoting a stable butyrate producing colonic ecosystem decrease the rate of aberrant crypt foci in rats. *Gut* **48**, 53-61 (2001).

11 Pierre, F. *et al.* Short-chain fructo-oligosaccharides reduce the occurrence of colon tumors and develop gut-associated lymphoid tissue in Min mice. *Cancer research* **57**, 225-228 (1997).

12 Buecher, B. *et al.* Fructooligosaccharide associated with celecoxib reduces the number of aberrant crypt foci in the colon of rats. *Reproduction, nutrition, development* **43**, 347-356 (2003).

13 Corpet, D. E. & Pierre, F. Point: From animal models to prevention of colon cancer. Systematic review of chemoprevention in min mice and choice of the model system. *Cancer epidemiology, biomarkers & prevention : a publication of the American Association for Cancer Research, cosponsored by the American Society of Preventive Oncology* **12**, 391-400 (2003).

14 Caderni, G. *et al.* Slow-release pellets of sodium butyrate do not modify azoxymethane (AOM)-induced intestinal carcinogenesis in F344 rats. *Carcinogenesis* **22**, 525-527 (2001).

15 Asanuma, N. *et al.* Characterization and transcription of the genes involved in butyrate production in Butyrivibrio fibrisolvens type I and II strains. *Current microbiology* **51**, 91-94, doi:10.1007/s00284-005-4477-x (2005).

16 Trottier, M. *et al.* Enhanced production of early lineages of monocytic and granulocytic cells in mice with colitis. *PNAS* **109**, 16594-9 (2012).
17 Hall, L. *et al*. Induction and activation of adaptive immune populations during acute and chronic phases of a murine model of experimental colitis. *Dig. Dis. Sci.* **56**, 79-89 (2011)
18 Yoshioka, K. *et al.* Role of natural killer T cells in the mouse colitis-associated colon cancer model. *Scand. J Immunol.* **75**, 16-26 (2011).
19 Waddell, A. *et al.* Colonic eosinophilic inflammation in experimental colitis is mediated by Ly6C(high) CCR2(+) inflammatory monocyte/macrophage-derived CCL11. *J. Immunol*. **186**, 5993-6003 (2011).
20 Cox, J. *et al.* Opposing consequences of IL-23 signaling mediated by innate and adaptive cells in chemically induced colitis in mice. *Mucosal Immunol.* **5**, 99-109 (2012)
21 Horino, J. *et al*. Suppressor of cytokine signaling-1 ameliorates dextran sulfate sodium-induced colitis in mice. *Int. Immunol.* **20**, 753-762 (2008). 1-14 15